Received: 18 October 2022 | Revised: 1 February 2023 | Accepted: 2 February 2023

DOI: 10.1002/hyp.14823

SCIENTIFIC BRIEFING

HP TODAY WILEY

Spatial downscaling of precipitation for hydrological modelling: Assessing a simple method and its application under climate change in Britain

Alison L. Kay | Alison C. Rudd | James Coulson

UK Centre for Ecology & Hydrology, Wallingford, UK

Correspondence
Alison L. Kay, UK Centre for Ecology & Hydrology, Wallingford OX10 8BB, UK.
Email: alkay@ceh.ac.uk

Funding information
Natural Environment Research Council, Grant/Award Number: NE/S017380/1

Abstract

National or regional grid-based hydrological models are usually run at relatively fine spatial resolutions. But the meteorological data necessary to drive such models are often coarser resolution, so some form of spatial downscaling is generally required. A 1 km hydrological model for Great Britain is used to test the performance of a simple method of downscaling precipitation based on 1 km patterns of long-term mean annual rainfall (Standard Average Annual Rainfall; SAAR). For a range of coarser resolutions (5, 10, 25 and 50 km), a 1 km grid of multiplicative scaling factors is derived as the ratio of the 1 km grid box SAAR divided by the mean SAAR of the coarser resolution grid box that contains it. A dataset of 1 km daily observation-based precipitation is then degraded to the coarser resolutions, and application of SAAR scaling factors is compared to no downscaling and direct use of 1 km data, for simulating river flows for a large set of catchments. SAAR-based downscaling provides a clear improvement over no downscaling. Using monthly rather than annual long-term mean rainfall patterns provides minimal further improvement. There are no strong relationships between performance and catchment properties, but performance using 50 km precipitation without downscaling tends to be worse for smaller, steeper catchments and those with a more south-westerly aspect; these benefit more from SAAR-based downscaling. An assessment using high-resolution convection-permitting model data shows relatively small changes in derived SAAR scaling factors between a baseline and far-future period, suggesting that use of historical scaling factors for future periods is reasonable. Applicability of this simple downscaling method for other parts of the world should be similarly assessed, for both historical and future periods. While use of annual patterns seems to be sufficient in Britain, areas where spatial rainfall patterns are more variable through the year may require use of sub-annual patterns.

KEYWORDS
convection-permitting model, hydrology, precipitation, rainfall, rainfall-runoff model, spatial downscaling

1 | INTRODUCTION

Global hydrological models are usually run at relatively coarse scales (~0.5–1°), although efforts are underway to develop so-called 'hyper-resolution' models (0.1–1 km; Bierkens et al., 2015). However, national- or regional-scale hydrological models typically require such finer resolutions, to better represent the local detail of particular areas and river networks. Examples of national- or regional-scale grid-based hydrological models include; the Grid-to-Grid (G2G) model (usually 1 km resolution, Bell et al., 2009, Kay et al., 2021), the WaSIM-ETH model (typically 1 km; Kleinn et al., 2005), the mHM model (resolution ~1–50 km; Thober et al., 2018), and the Hebei model (resolution 1–9 km, Tian et al., 2020). Models based on hydrological response units, rather than grids, can also have fine spatial scales (e.g., Coxon et al., 2019; Skaugen, 2002).

The meteorological data required to drive hydrological models typically includes precipitation and potential evaporation (PE), plus (at least) temperature if a snow module is included. However, gridded meteorological data are often at a coarser spatial resolution than required by national or regional grid-based hydrological models (e.g., Gagnon et al., 2012; Maina et al., 2020). For example, ERA5 re-analysis data is ~30 km resolution, (ecmwf.int/en/forecasts/datasets/reanalysis-datasets/era5), and global and regional climate models (GCMs/RCMs) typically have resolutions of tens of kilometres (e.g., the latest UK Climate Projections, UKCP18, include GCM data at 60 km resolution and RCM data at 12 km resolution; Murphy et al., 2018). The same issue applies for finer-scale land-surface modelling (e.g., Fiddes & Gruber, 2014; Martinez-de la Torre et al., 2018), although a wider range of driving variables is typically then required (Robinson et al., 2020a). Some form of spatial downscaling is thus required to use such datasets for hydrological or land-surface modelling (some form of bias-correction may also be desired, but this essentially separate issue is not considered here).

For downscaling temperature data, a lapse rate can be used alongside often readily available finer-scale elevation data (e.g., Bell et al., 2016; Kleinn et al., 2005; Perra et al., 2020; Robinson et al., 2017), as there is typically a strong relationship between elevation and temperature. PE is highly seasonally predictable and significantly less (spatially and temporally) variable than precipitation (Calder et al., 1983), and river flows are generally less sensitivity to errors in PE than in precipitation (e.g., Kay et al., 2013; Manning et al., 2009), thus relatively simple PE data are often considered sufficient to close the water balance in hydrological models (e.g., Boughton, 2006; Oudin et al., 2005). Consequently, PE data can generally be copied down to a finer-scale spatial grid without significant loss of model performance for river flows (e.g., Bell et al., 2016; Lane et al., 2022). Alternatively, some form of statistical downscaling can be used (e.g., Yang et al., 2005), or the meteorological variables required to estimate PE can be downscaled before use (e.g., Robinson et al., 2017, 2020b).

Appropriate downscaling of precipitation is more important for hydrological modelling. Sampson et al. (2020) show that use of coarse-scale (0.125°) gridded precipitation data leads to large errors in the water balance compared to use of point-scale data, for locations across the United States with a range of climate regimes and soil types. They state that 'hyperresolution modelling at continental to global scales may produce inaccurate predictions if there is not parallel effort to produce higher resolution precipitation inputs or sub-grid precipitation parameterizations'. There are many possible ways to downscale precipitation data, ranging from complex statistical disaggregation methods (e.g., Gagnon et al., 2012; Sharma et al., 2007; Skaugen, 2002), to regression-based methods (e.g., Kara & Yucel, 2015; Sharifi et al., 2019), to much simpler methods based on typical rainfall patterns (e.g., Fiddes & Gruber, 2014; Früh et al., 2006; Kleinn et al., 2005; Marke et al., 2011). The more complex methods can be time-consuming to setup (e.g., requiring more ancillary data and potentially subjective choices on what to include) and more difficult to apply (e.g., requiring the full downscaled dataset to be produced prior to running the hydrological model), whereas simpler methods are more straightforward in terms of setup (e.g., requiring less ancillary data and few, if any, choices) and application (e.g., they can be applied during the hydrological modelling process), but less flexible.

Past applications of the G2G hydrological model for GB have used spatial patterns of Standard Average Annual Rainfall (SAAR) data for 1961–1990, available on a 1 km grid across Britain (catalogue.ceh.ac.uk/documents/2a2b1b05-a30f-4e04-9b37-75fa5ef5c26bht), to downscale coarser resolution precipitation data (Bell et al., 2007a). For each 1 km grid box, a scaling factor is calculated as the ratio of the 1 km SAAR divided by the mean SAAR of the coarser resolution grid box that contains it. This is used as a multiplication factor to downscale the coarser resolution precipitation time-series to the finer-scale grid. This method has been used with observation-based data (e.g., Met Office 5 km rainfall data; Bell et al., 2007a, 2016) and with RCM data at various resolutions (e.g., 12 km, Lane & Kay, 2021, Robinson et al., 2022; 25 km, Bell et al., 2007b, 2016, Rudd et al., 2019; 50 km, Kay et al., 2018), and a variation has been used to make catchment-average RCM data (Kay et al., 2006). A similar approach is used for downscaling climate model data by Kleinn et al. (2005) over Germany, and by Früh et al. (2006) and Marke et al. (2011) for the upper Danube catchment, which includes part of the Alps.

The aims of this paper are to

1. demonstrate the performance of the simple SAAR-based precipitation downscaling method for hydrological modelling, for a large set of catchments across GB, and
2. assess the applicability of historically-derived SAAR scaling factors for use in future periods, for hydrological climate change impact studies.

To demonstrate the performance of the method for hydrological modelling, a 1 km daily observation-based precipitation dataset is degraded to a range of coarser spatial resolutions, then use of the SAAR-based downscaling method is compared against use of degraded precipitation data, and against direct use of the original 1 km precipitation data, for simulating river flows across Britain. This allows comparison of differences in performance due solely to

precipitation spatial resolution and downscaling. Performance of a simple extension of the method, using patterns of Standard Average Monthly Rainfall (SAMR), is similarly assessed. The variation in performance of SAAR-based downscaling for catchments with different properties is also investigated. To assess the applicability of historically derived SAAR ratios for use in future periods, data from a very high resolution Convection-Permitting Model (CPM) are used to derive and compare SAAR scaling factors for a historical baseline time-slice (1980–2000) and a far-future time-slice (2060–2080).

2 | METHODS

2.1 | Precipitation data

The historical assessment uses 1 km daily observation-based precipitation from CEH Gridded Estimates of Areal Rainfall (CEH-GEAR; Tanguy et al., 2016, Keller et al., 2015). CEH-GEAR rainfall estimates are derived from UK rain gauge network precipitation totals, using natural neighbour interpolation and a normalization step based on average annual rainfall, and were developed to provide reliable 1 km grids of daily and monthly rainfall across the UK to support hydrological modelling. These data are degraded (averaged up) to a range of coarser resolutions; 5, 10, 25, and 50 km. In each case, three options for converting data back to the 1 km grid are then applied:

1. Copy the data back down to the 1 km resolution, by simply taking data for each 1 km pixel from the coarser resolution box within which it sits. This option is hereafter termed 'without downscaling' (or 'wo_d');
2. Copy the data back down to the 1 km resolution and multiply by a SAAR scaling factor (the ratio of the SAAR of the 1 km grid box to the average SAAR across the coarser resolution grid box within which it sits). This option is hereafter termed 'with SAAR-based downscaling' (or 'w_saard').
3. Copy the data back down to the 1 km resolution and multiply by a SAMR scaling factor (the ratio of the SAMR of the 1 km grid box to the average SAMR across the coarser resolution grid box within which it sits, calculated separately for each of the 12 months of the year). This option is hereafter termed 'with SAMR-based downscaling' (or 'w_samrd').

The data from each combination of resolution and downscaling option above is used to drive a national-scale grid-based hydrological model for GB (Section 2.2). The CEH-GEAR 1 km daily precipitation data are also used directly to drive the hydrological model (hereafter 'direct_1km'), as a benchmark of performance.

It should be noted that the SAAR and SAMR scaling factors for a given 1 km grid box will obviously vary depending on the positioning of the coarser resolution grid. Only one position of each coarser resolution grid has been tested here; that with the bottom left corner at GB national grid coordinate 0 Easting and 0 Northing. It should also be noted that, by definition, the mean of the SAAR or SAMR ratios across each coarser resolution grid box is equal to 1, so the total amount of precipitation across the area is the same with or without downscaling.

Figure 1 presents SAAR maps, showing the typical distribution of annual rainfall across GB, and maps and boxplots of the 1 km grids of SAAR scaling factors (SAAR ratios), for each degraded precipitation resolution (5, 10, 25 and 50 km). The maps show that the spatial variation in SAAR ratios is greater in hillier areas to the north and west of Britain than in the flatter regions to the south/east of the country. The boxplots show that the range of SAAR ratio values increases for the coarser resolutions. The median value across GB also decreases slightly for the coarser resolutions; this seems to be because the (typically higher altitude) areas where the SAAR ratios are greater than 1 are more concentrated than those where the SAAR ratios are less than 1.

Figure 2 presents maps and boxplots of the 1 km grids of SAMR scaling factors (SAMR ratios) for each month, for precipitation degraded to 50 km resolution. The maps show that the spatial pattern of SAMR ratios is similar for each month. The boxplots show very similar median values for each month, but with lower variability for summer months than winter months, perhaps because of a higher occurrence of strong cyclonic weather types in winter than summer (Pope et al., 2022). The corresponding 1:50 km SAAR ratios (Figure 1) have a similar variability to the SAMR ratios for spring and autumn months (Figure 2).

Using UKCP18 GCM data, Pope et al. (2022) show that future large-scale circulation changes for GB tend towards an increase in weather types associated with cyclonic and westerly winds in winter, whereas in summer there is an increase in dry settled weather types and a reduction in the wet/windy weather types. Such changes in typical weather patterns could affect SAAR and SAMR ratios for future periods. Thus, the applicability of historically derived SAAR ratios for future periods is assessed, using the UKCP18 Local projections (Kendon et al., 2021). These projections comprise a 12-member ensemble of the Hadley Centre CPM, nested in an RCM perturbed-parameter ensemble (PPE), for three 20-year periods (December 1980–November 2000, December 2020–November 2040 and December 2060–November 2080) under RCP8.5 emissions. The data are available on their ~2.2 km rotated lat-lon grid, but also re-projected to a 5 km grid aligned with the GB national grid (Met Office Hadley Centre, 2019); the re-projected 5 km CPM precipitation data are used here (see Section 2.5).

2.2 | Hydrological modelling

The Grid-to-Grid (G2G) is a grid-based runoff-production and routing model that typically uses a 1 km grid and a 15-min time-step across GB (Bell et al., 2009). The optional snow module (Bell et al., 2016) is applied here. River flows simulated by G2G perform well for a wide range of catchments (Bell et al., 2009, 2016; Formetta et al., 2018; Rudd et al., 2017), particularly where the flow regime is relatively unaffected by artificial influences as the model essentially simulates natural, rather than gauged, flows.

Daily 1 km precipitation is divided equally over each model time-step within a day. Monthly 40 km grids of short grass PE (MORECS;

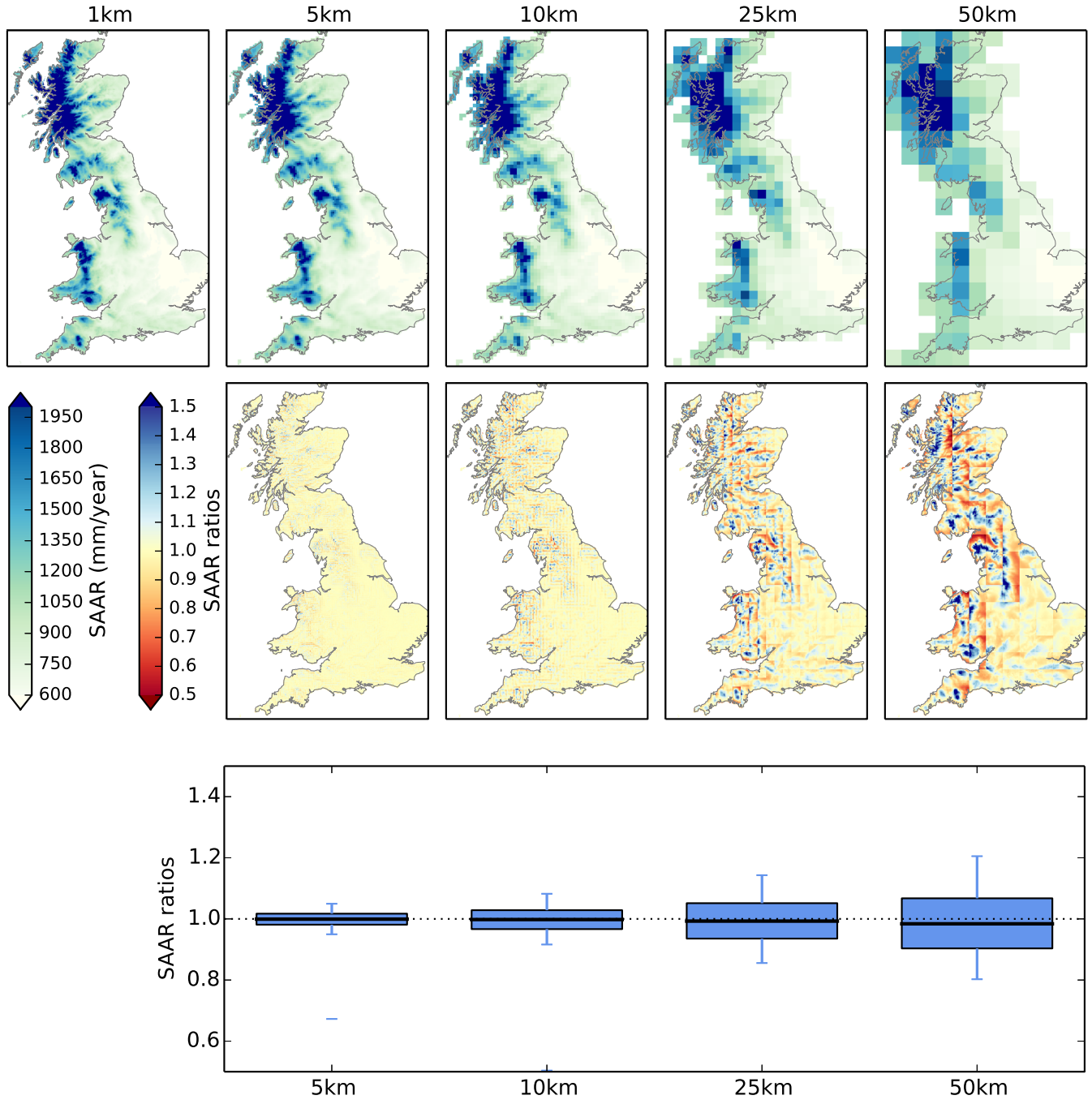

FIGURE 1 Maps of the SAAR values (mm/year) across GB (top row), maps of the SAAR scaling factors (ratios) on the 1 km grid (middle row), and boxplots showing the SAAR ratio ranges (bottom), for each degraded precipitation resolution (5, 10, 25 and 50 km). The boxes show the 25th–75th percentile range, the line across the box shows the median, the whiskers show the 10th–90th percentile range, and dashes beyond the whiskers show the overall min and max (if within the plotted range)

Hough & Jones, 1997) are copied down to the 1 km grid and divided equally over each model time-step within a month. Daily 1 km grids of min and max temperature (Met Office et al., 2019) are interpolated through the day using a sine curve (Kay & Crooks, 2014).

Simulations are run for October 1980–December 2010 for each precipitation option described in Section 2.1. The simulations were all initialised using the same states file, saved from the end of a prior simulation using 1 km precipitation. Outputs were only analysed for January 1981–December 2010 (i.e., October–December 1980 was treated as a spin-up).

2.3 | Performance of downscaling methods

The model outputs time-series of daily mean river flows for selected 1 km pixels corresponding to gauged catchments in the National River

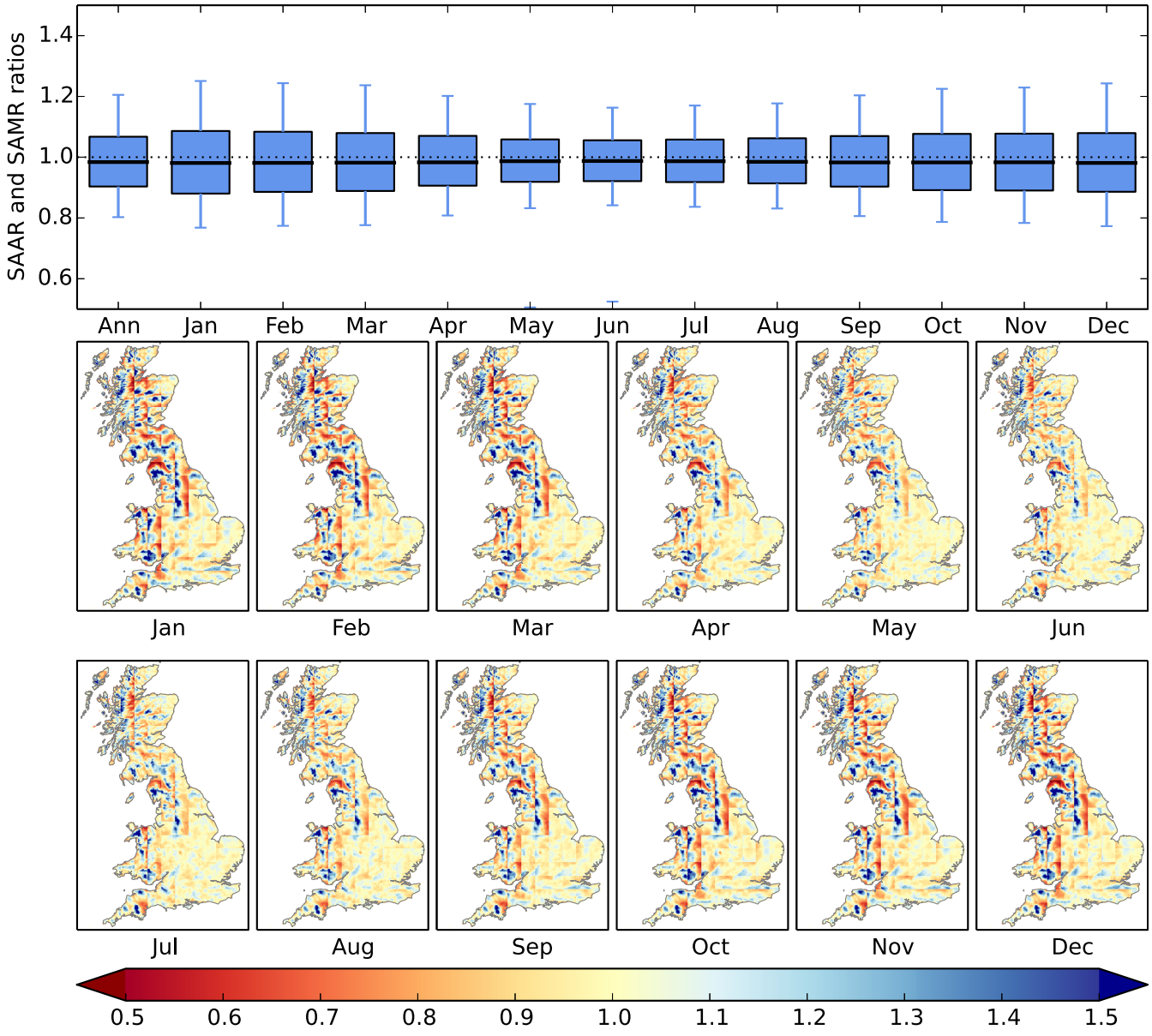

FIGURE 2 Boxplots and maps showing the SAMR scaling factors (ratios) for each month on the 1 km grid, for precipitation degraded to 50 km resolution. Also shown as a boxplot are the corresponding 1:50 km SAAR ratios ('Ann', left), for comparison

Flow Archive (NRFA; ceh.ac.uk/data/nrfa/). The performance of the various spatial rainfall processing options is assessed by calculating several performance measures comparing simulated and observed flows (for January 1981–December 2010), for a large set of catchments across GB (Figure 3). The 831 catchments included in the assessment have an area of at least 50 km^2, and less than 50% missing data in the required period.

The performance measures include the standard Nash-Sutcliffe efficiency (NS, Equation 1, which focuses more on high flows), Nash–Sutcliffe using the square-root of flows (NSroot, which focuses more on average flows), Nash–Sutcliffe using the natural logarithm of flows (NSlog, which focuses more on low flows) (e.g., Rudd et al., 2017), as well as overall Bias (Equation 2).

$$\mathrm{NS} = 1 - \frac{\sum (Q_{obs} - Q_{sim})^2}{\sum (Q_{obs} - \overline{Q_{obs}})^2} \quad (1)$$

$$\mathrm{Bias} = 100 \left(\frac{\overline{Q_{sim}}}{\overline{Q_{obs}}} - 1 \right) \quad (2)$$

For the Nash–Sutcliffe measures, a value of 1 signifies perfect performance, while a value less than zero indicates performance worse than that of mean flow. For the Bias measure, a value of zero indicates perfect performance, while positive values indicate over-estimates and negative values are under-estimates.

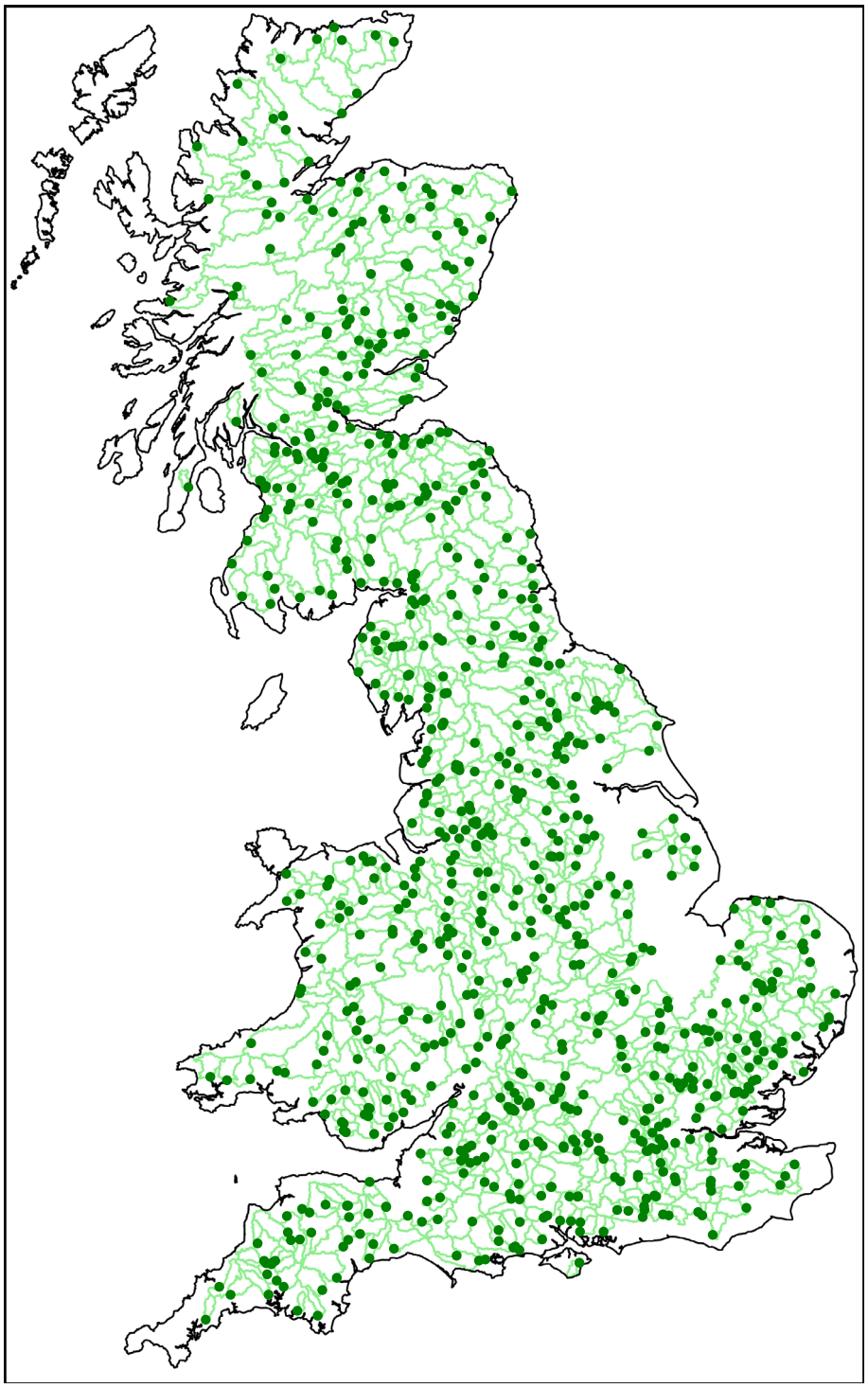

FIGURE 3 The 831 catchments used to assess performance

2.4 | Performance relative to catchment properties

Scatter plots are used to assess relationships between performance differences and various catchment properties taken from the NRFA (nrfa.ceh.ac.uk/feh-catchment-descriptors). This is done both to assess the types of catchment which perform worse when no downscaling is applied (performance values from use of data at 50 km resolution 'wo_d' minus values from 'direct_1km'), and those which benefit most from the application of SAAR-based downscaling (performance values from use of data at 50 km resolution 'w_saard' minus 'wo_d'). Note that, for the Bias measure, the difference in the absolute value is calculated. The catchment properties used are catchment drainage area ('Area'; km^2), mean drainage path slope ('dpsbar', m/km), and mean aspect ('aspbar'; degrees), although since the Area distribution is highly skewed, with few large catchments, $\log_{10}$Area is used (Figure S1). The aspbar property takes values between 0° and 360°, with 0° (=360°) northwards, 90° eastwards, 180° southwards, and 270° westwards. There are no strong dependencies between

these catchment properties, although large catchments tend to have shallower slopes and a more easterly aspect (Figure S1).

To better highlight potential relationships, a best fit line is derived for each combination of performance measure and catchment property. A linear fit is used for $\log_{10}$Area and dpsbar, but since aspbar values are circular a sinusoid of the form $A + B^{*}sin(aspbar_{rad} + C)$ is fitted, where $aspbar_{rad}$ is the aspbar values converted from degrees to radians. In each case, the fitting excludes outliers by only using points where the y values have a *z*-score <3 (i.e., those within three standard deviations of the mean).

2.5 | Downscaling for future time-slices

Grids of 5 km CPM time-slice mean annual total precipitation are used ('ann-20y' from Met Office Hadley Centre, 2019), for the baseline period (December 1980–November 2000) and the far-future period (December 2060–November 2080). These are averaged up to 50 km resolution, then 5 km SAAR-ratio grids are calculated (the ratio of the SAAR of the 5 km grid box to the average SAAR across the 50 km resolution grid box which contains it). Maps of the baseline 5:50 km SAAR ratios for each CPM ensemble member (Figure S3) all look very similar to each other and to the map of observation-based 1:50 km SAAR ratios in Figure 1. The baseline and far-future SAAR-ratio grids are compared, to assess any potential changes due to climate change. The assessment looks at

1. If 5 km grid boxes are more likely to see increases/decreases in far-future SAAR ratios according to whether their baseline SAAR ratios are above or below 1;
2. If 5 km grid boxes located in particular quadrants (SW, NW, NE, SE) of each 50 km grid box are more likely to see increases/decreases in SAAR ratios in the far-future. Each quadrant comprises the 5 x 5 set of 5 km grid boxes located in the given direction from the centre of the 50 km grid box.

As well as looking at the above across the whole of GB, the analysis looks at whether there are differences according to location within GB, by using a simple West/East split of 50 km grid boxes, and a simple North/South split of 50 km grid boxes. The general analysis pools all 12 CPM ensemble members together, but the scale of the variation between ensemble members is also shown.

3 | RESULTS

3.1 | Performance of downscaling methods

Boxplots of the performance measure ranges at each degraded resolution show that SAAR- and SAMR-based downscaling improves performance over no downscaling, bringing it back towards the performance of using the 1 km data directly (Figure 4). However, the performance without downscaling falls off relatively slowly, with little difference seen at 5 and 10 km resolutions. At 25 km resolution, the performance without downscaling starts to reduce, with worse performance at 50 km resolution. In both cases, the use of SAAR-based downscaling improves the performance significantly, particularly for overall bias. The use of SAMR-based downscaling provides only a small further improvement, for the NSlog measure (i.e., low flows).

Scatter plots directly comparing the performance without downscaling and with SAAR- and SAMR-based downscaling from 50 km resolution, to direct use of 1 km data, show a clearly better match from use of downscaling (Figure 5). Pearson correlation coefficients are in the range 0.894–0.981 without downscaling, but increase to 0.996–0.999 with SAAR-based downscaling. The greatest improvement is seen for the Bias measure. There is a small further improvement for each measure when using SAMR-based downscaling, with Pearson *r* in the range 0.998–0.999.

3.2 | Performance relative to catchment properties

While there are no strong relationships between performance differences and catchment properties (Figure S2), performance at 50 km resolution without downscaling tends to be worse (compared to direct use of 1 km data) for smaller catchments, steeper catchments, and catchments with a more south-westerly aspect. This is because smaller or steeper catchments are more likely to experience differing typical rainfall than neighbouring catchments, due to the influence of orography on local weather patterns. Similarly, since the predominant direction of weather fronts in the United Kingdom is from the south-west, catchments with a more south-westerly aspect will experience differing typical rainfall compared to neighbouring catchments to the leeward side of elevated areas.

Satisfyingly, performance at 50 km resolution with SAAR-based downscaling (compared to 50 km without downscaling) shows the greatest improvement for smaller or steeper catchments and those with a more south-westerly aspect (Figure 6). Note that the linear best fit lines plot as non-linear because of the log scale on the catchment property axes, and that the exclusion of outliers from the calculation of the best fit lines only has a significant effect on those for the NS measure (not shown).

3.3 | Downscaling for future time-slices

Boxplots summarizing the percentage changes in CPM-derived SAAR ratios between the baseline and far-future periods show only small differences according to whether the baseline SAAR ratios are above or below 1 (when pooled over the 12 CPM ensemble members, Figure 7). For GB as a whole, there a slight tendency towards a decrease in the SAAR ratio in grid boxes where the baseline value is above 1, and an increase in the SAAR ratio in grid boxes where the baseline value is below 1, but this does not hold for all CPM ensemble members (plus signs in Figure 7). This result is similar when split by West/East 50 km grid boxes, but when split by North/South 50 km

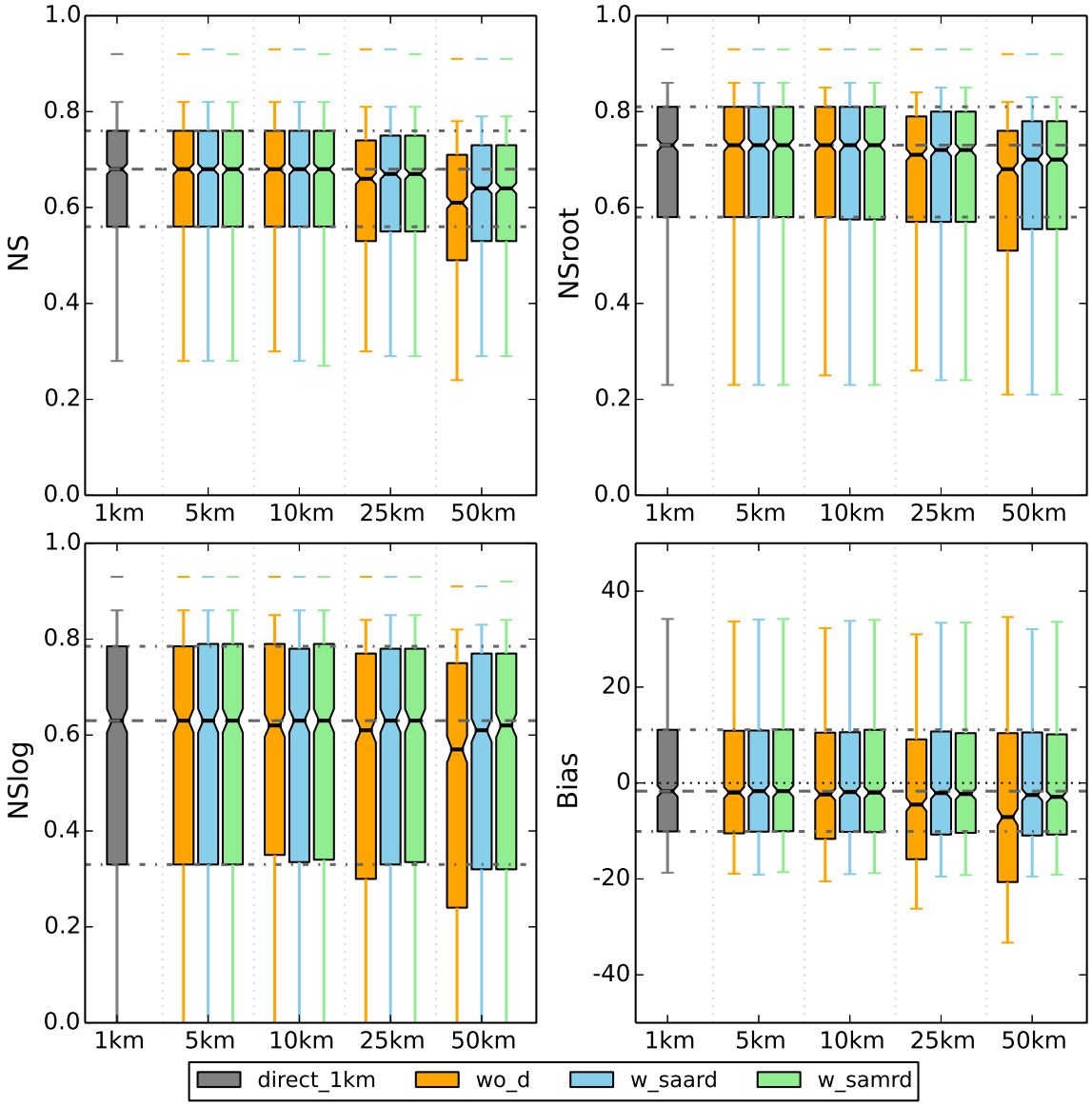

FIGURE 4 Summary of performance without downscaling ('wo_d)', with SAAR-based downscaling ('w_saard') and with SAMR-based downscaling ('w_samrd') for 5, 10, 25 and 50 km resolutions, compared to direct use of 1 km data ('direct_1km'). The boxes show the 25th–75th percentile range across the set of catchments, with the median shown by the line across the box. The whiskers show the 10th–90th percentile range, with overall min and max shown by dashes beyond the whiskers (if within the plotted range)

grid boxes the more Northern boxes show a stronger pattern of decrease where the baseline value is above 1 and increases where the baseline value is below 1. The median changes for the 12 individual CPM ensemble members indicate that the penultimate CPM ensemble member (13) shows quite different changes in SAAR ratios to the rest. Maps of the changes in SAAR ratios (far-future minus baseline) for each CPM ensemble member also show some differences between ensemble members (Figure S3).

Boxplots summarizing the baseline to far-future percentage changes in CPM-derived SAAR ratios by quadrant show clearer differences (when pooled over the 12 CPM ensemble members, Figure 8). For GB as a whole, there a tendency towards an increase in the SAAR ratio in 5 km grid boxes located in the SW or NW quadrants of their 50 km grid box, and a decrease in the SAAR ratio in 5 km grid boxes located in the NE or SE quadrants of their 50 km grid box. This pattern is more accentuated for West rather East 50 km grid boxes, and for North rather than South 50 km grid boxes. In the West 50 km grid boxes in particular, the median changes for the 12 CPM ensemble members (plus signs in Figure 8) show the same sign.

4 | DISCUSSION

The performance of a simple method of precipitation downscaling for hydrological modelling, based on use of patterns of long-term mean annual rainfall (SAAR), has been demonstrated for a large set of

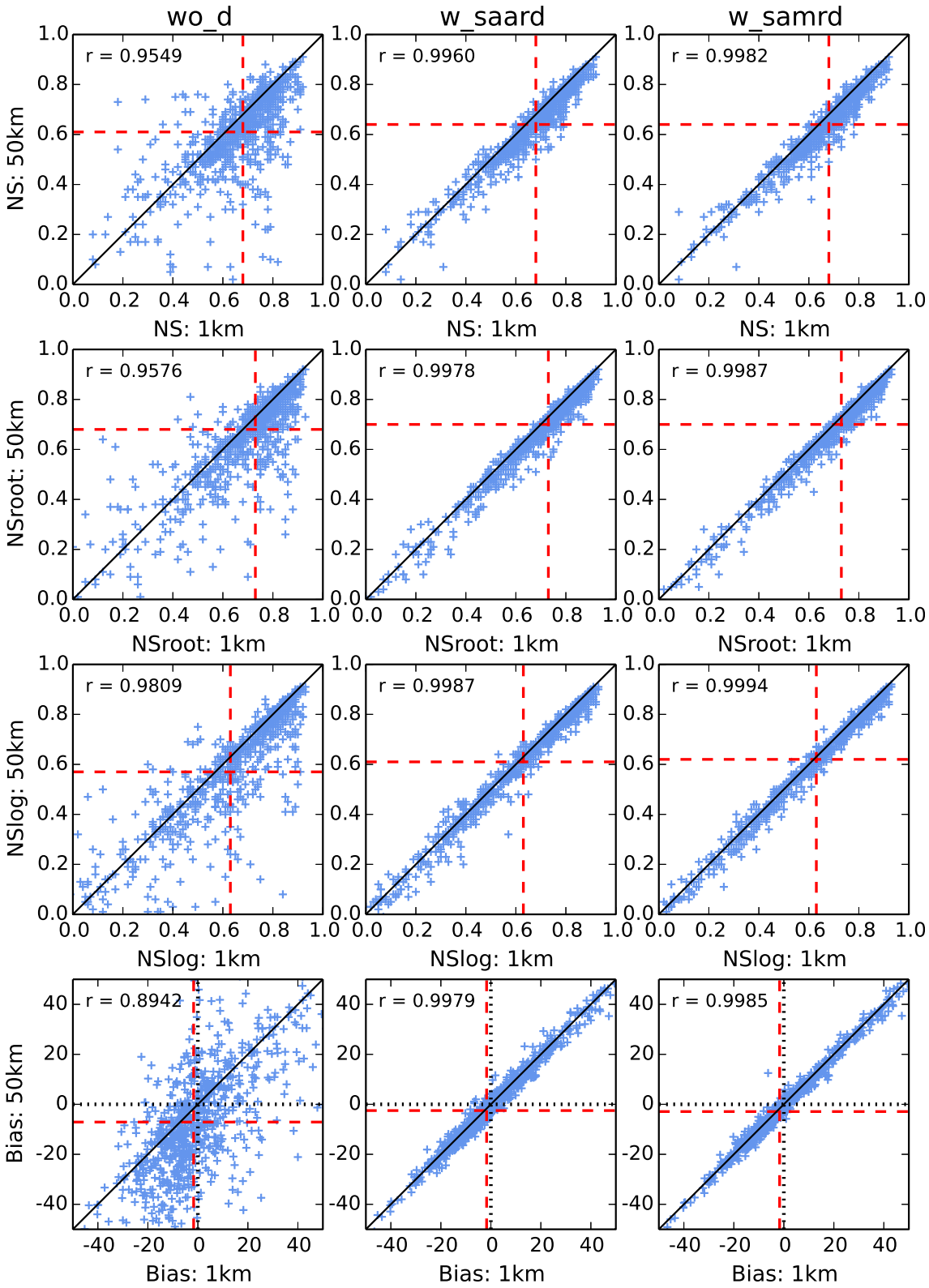

FIGURE 5 Scatter plots showing the performance without downscaling ('wo_d', left), with SAAR-based downscaling ('w_saard', middle) and with SAMR-based downscaling ('w_samrd', right) from 50 km resolution (*y*-axis), versus direct use of 1 km data (*x*-axis). The median performance in each case is shown by the red dashed lines. The Pearson correlation coefficient *r* is given to the top-left of each plot

catchments across Great Britain (Section 3.1). The method provides a clear improvement over simply copying coarse resolution (10, 25 or 50 km) precipitation down to the resolution required by the hydrological model (1 km). However, overall performance of SAAR-based downscaling from 50 km resolution is not quite as good as that from direct use of 1 km data. A minimal further improvement is

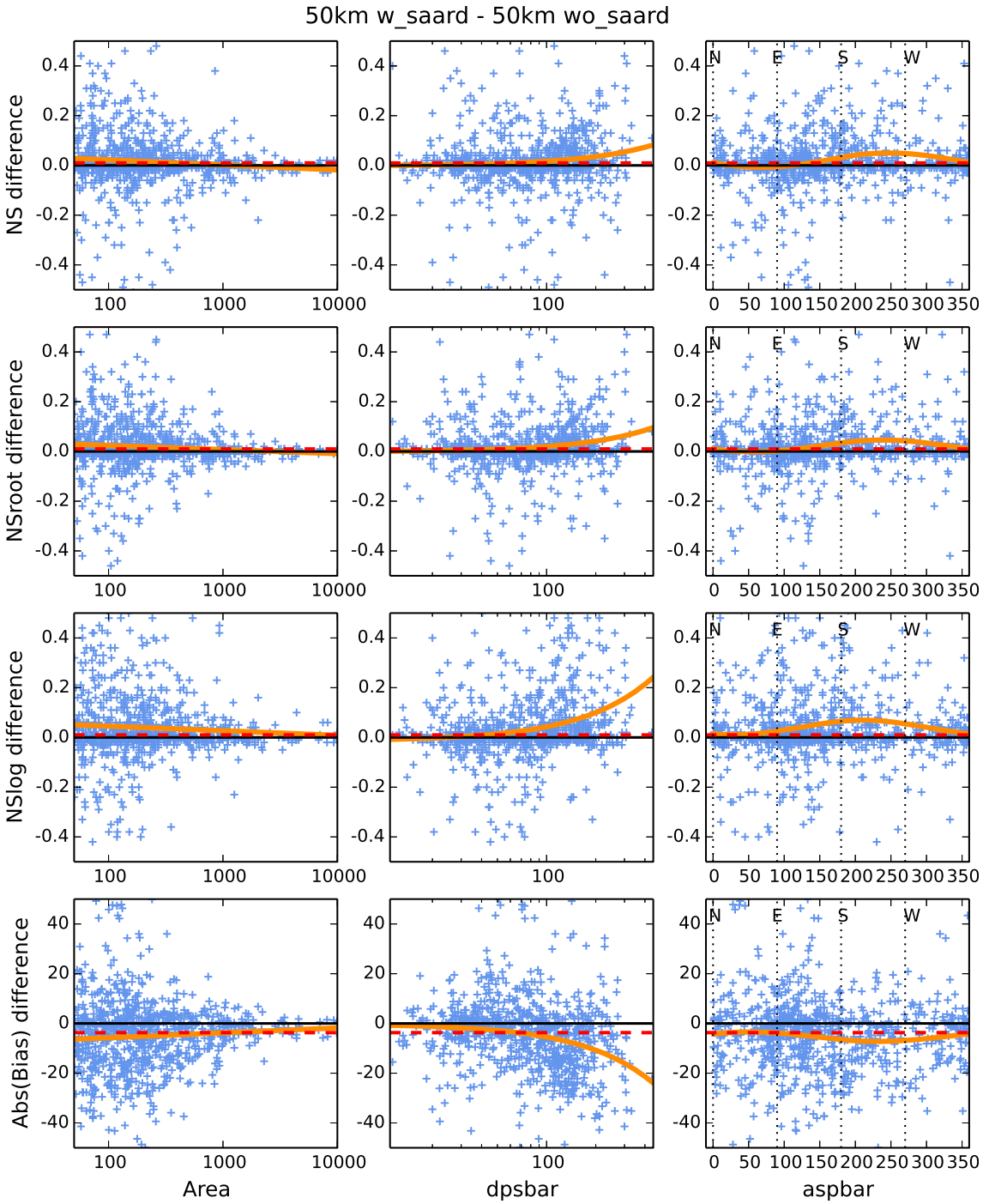

FIGURE 6 Scatter plots showing the relationship between catchment properties (*x*-axis) and the difference in the four performance measures from use of data at 50 km resolution with SAAR-based downscaling and without downscaling (*y*-axis). The catchment properties (left to right) are the log of the catchment drainage area (Area, km^2), mean drainage path slope (dpsbar; m/km), and mean aspect (aspbar, °). Note that Area and dpsbar are plotted on log scales. Also shown is the median performance difference (red dashed horizontal line) and a best fit line (orange solid line; see Section 2.4)

provided by use of monthly rather than annual patterns of long-term mean rainfall, likely due to the predominance in Britain of frontal rainfall systems coming from the west throughout the year (Pope et al., 2022; metoffice.gov.uk/weather/learn-about/weather/atmosphere/weather-fronts).

Analyses of performance relative to catchment properties shows that, while there are no strong relationships, performance using 50 km precipitation data without any downscaling tends to be worse for smaller, steeper catchments, and catchments with a more south-westerly aspect (Section 3.2). This is also likely to be related to

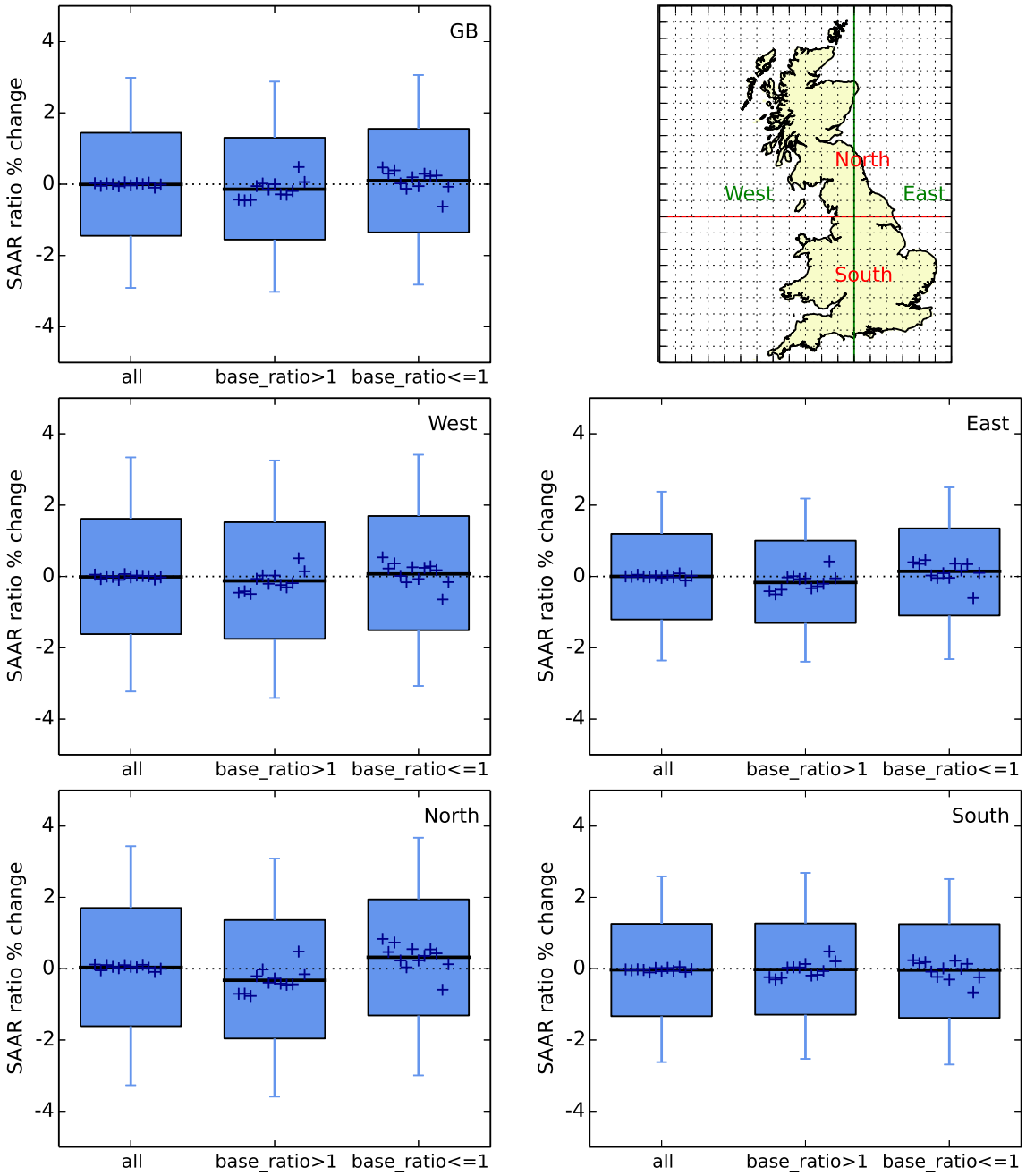

FIGURE 7 Boxplots showing the range of the percentage change in the 5 km SAAR-ratio grids, for all land 5 km grid boxes ('all'), and split by grid boxes where the SAAR-ratio for the baseline period is greater than 1 ('base_ratio>1') or otherwise ('base_ratio<=1'). The top-left plot shows the results over GB, while the middle pair of plots shows the results over the West/East of GB, and the bottom pair of plots shows the results over the North/South of GB. The West/East and North/South divisions are show in the map (top-right). In each case, the boxes show the 25th–75th percentile range across the CPM ensemble, with the median shown by the line across the box, the whiskers show the 10th–90th percentile range. The plus signs show the medians for each CPM ensemble member separately (in order of ensemble member number, left to right)

predominant rainfall systems, and so performance with SAAR-based downscaling shows the greatest improvement for these same types of catchment. However, the performance assessment presented here only includes catchments with an area of at least 50 km^2, due to the use of daily precipitation data. Use of the method for smaller catchments, perhaps with sub-daily precipitation data, would need further consideration.

An assessment using data from a convection-permitting model (CPM) ensemble for the UK shows relatively small changes (typically ±2%) in derived 5:50 km SAAR downscaling factors between baseline (1980–2000) and far-future (2060–2080) periods (Section 3.3). There tends to be an increase in westerly quadrants and a decrease in easterly quadrants, which is consistent with the UKCP18 GCM analysis of Pope et al. (2022) showing an increase in occurrence of weather types

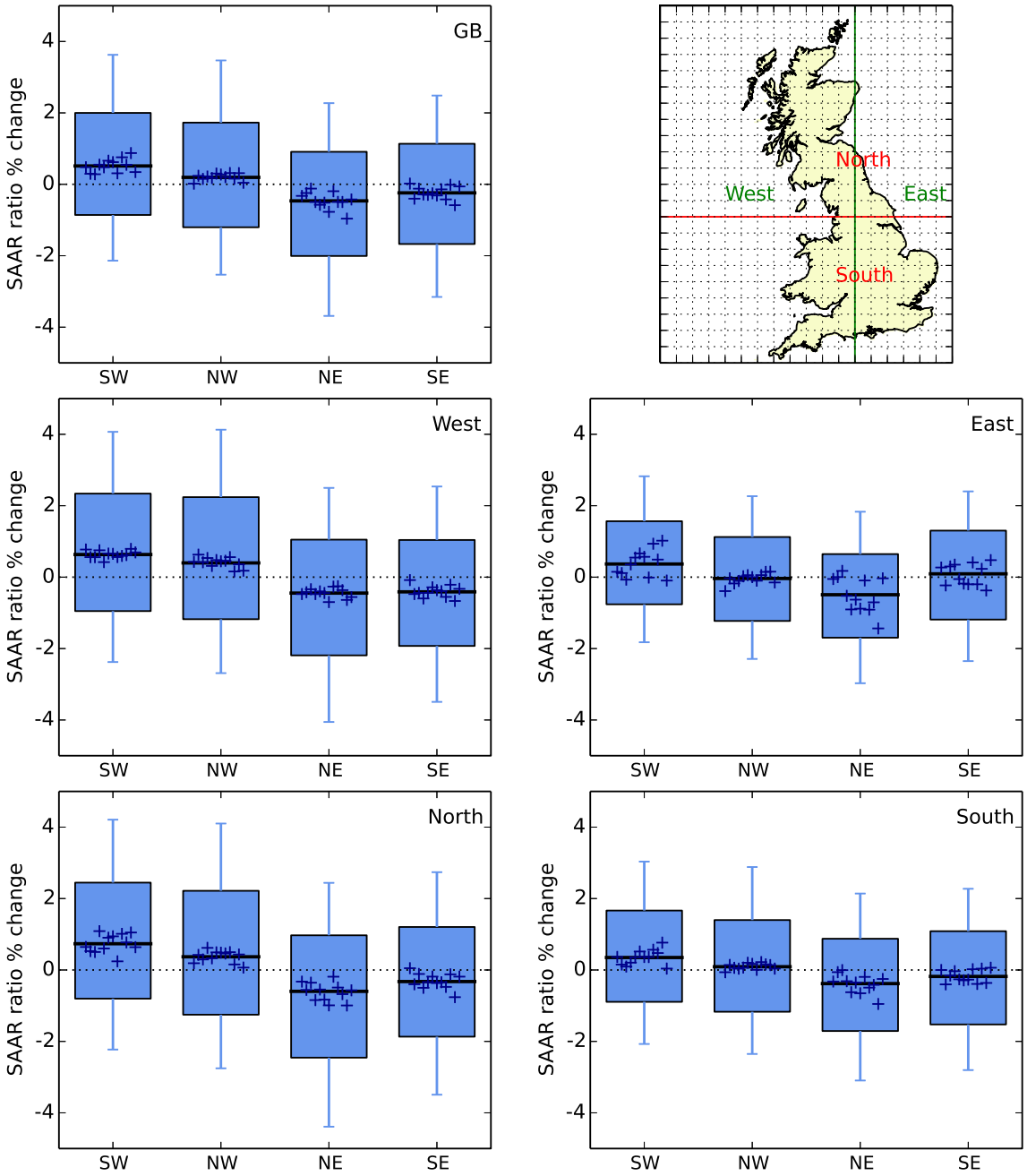

FIGURE 8 Boxplots showing the range of the percentage change in the 5 km SAAR-ratio grids, split by the 25 × 25 km quadrant within each 50 km grid box ('South-West', 'North-West', 'North-East', 'South-East'). The top-left plot shows the results over GB, while the middle pair of plots shows the results over the West/East of GB, and the bottom pair of plots shows the results over the North/South of GB. The West/East and North/South divisions are show in the map (top-right). In each case, the boxes show the 25th–75th percentile range across the CPM ensemble, with the median shown by the line across the box, the whiskers show the 10th–90th percentile range. The plus signs show the medians for each CPM ensemble member separately (in order of ensemble member number, left to right)

associated with cyclonic and westerly winds in winter. Overall though, the changes are small, suggesting that it is reasonable to use historically derived SAAR patterns for downscaling precipitation from climate change simulations for future periods. However, the analysis only uses CPM data from a single climate model (that of the Met Office Hadley Centre), and was limited to use of 20-year baseline and future periods rather than WMO-recommended 30-year periods. It would be informative to repeat the analysis for convection-permitting versions of other climate models, for example using multi-model ensembles under development across Europe (Coppola et al., 2020). If a particular climate model suggests large changes in the predominant rainfall systems across Britain, at least at some times of year, then it may be that the historical SAAR- or SAMR-based downscaling patterns would need to be adjusted for use in future periods for that

climate model. Schipper et al. (2011) develop an extended version of the simple factor-based downscaling method of Früh et al. (2006) for the upper Danube, adding a dependence on wind direction and speed that would allow for potential changes in future climates.

It should be noted that if bias correction of climate model data is also desired then spatial downscaling can be performed before or after bias correction (e.g., Kay, 2021; Kleinn et al., 2005; Robinson et al., 2022). The analysis of Skoulikaris et al. (2022) suggests that bias-correction (using empirical quantile mapping) followed by downscaling (using spatio-temporal kriging) may be preferable to the reverse ordering, but they only compare the effect of the ordering in one mountainous basin in Greece. Alternatively, coarse resolution climate model data can be simultaneously bias-corrected and downscaled (e.g., Mamalakis et al., 2017; Prudhomme et al., 2012), but this approach is less flexible as the effects of downscaling and bias-correction cannot be independently assessed.

5 | CONCLUSIONS

A simple method of downscaling precipitation for input to a fully distributed national-scale hydrological model has been shown to perform well for a large set of catchments across Great Britain. The method could be applied in other regions of the world, dependent on the availability of information on typical spatial patterns of precipitation (e.g., Kleinn et al., 2005). While use of annual patterns seems to be sufficient for GB, in areas where spatial patterns of rainfall are more variable through the year the use of sub-annual (e.g., monthly or seasonal) patterns is likely to be necessary. Testing the performance of the method in other regions where rainfall is highly seasonal and has larger spatial and temporal variations would be advisable, and comparing the performance of the simple method against that of more complex methods would be interesting.

Data from a convection-permitting model (CPM) ensemble for the United Kingdom has been used to assess the applicability of historically derived SAAR ratios for future periods. This showed relatively small changes in derived SAAR ratios, suggesting that it is reasonable to use historically derived patterns for downscaling precipitation from climate change simulations for future periods in Britain. Again though, the applicability of this conclusion for other regions would ideally be tested, and extended to more than one climate model. Where CPM data are not available, it may be possible to assess future applicability using coarser resolution data and evaluating, for example, large-scale circulation changes (e.g., Pope et al., 2022). Although CPMs use spatial resolutions much closer to those typically required for hydrological modelling, they are very expensive, both computationally and in terms of data storage requirements (Kay, 2022). Thus, methods for spatial downscaling will still be needed for modelling the potential impacts of climate change on river flows using ensembles of coarser resolution climate model data.

ACKNOWLEDGEMENTS

This work was supported by the Natural Environment Research Council award number NE/S017380/1 as part of the Hydro-JULES programme delivering National Capability. Thanks to UKCEH colleague Rosie Lane for comments on the draft manuscript, and to two anonymous reviewers for comments which helped to improve the manuscript.

DATA AVAILABILITY STATEMENT

The precipitation data that support the findings of this study are openly available in EIDC at https://catalogue.ceh.ac.uk/documents/dbf13dd5-90cd-457a-a986-f2f9dd97e93c (CEH-GEAR data), and on CEDA at https://catalogue.ceda.ac.uk/uuid/e304987739e04cdc960598fa5e4439d0 (CPM data).

ORCID

Alison L. Kay https://orcid.org/0000-0002-5526-1756

Alison C. Rudd https://orcid.org/0000-0001-5996-6115

REFERENCES

Bell, V. A., Kay, A. L., Davies, H. N., & Jones, R. G. (2016). An assessment of the possible impacts of climate change on snow and peak river flows across Britain. *Climatic Change*, *136*(3), 539–553. https://doi.org/10.1007/s10584-016-1637-x

Bell, V. A., Kay, A. L., Jones, R. G., & Moore, R. J. (2007a). Development of a high resolution grid-based river flow model for use with regional climate model output. *Hydrology and Earth System Sciences*, *11*(1), 532–549.

Bell, V. A., Kay, A. L., Jones, R. G., & Moore, R. J. (2007b). Use of a grid-based hydrological model and regional climate model outputs to assess changing flood risk. *International Journal of Climatology*, *27*(12), 1657–1671.

Bell, V. A., Kay, A. L., Jones, R. G., Moore, R. J., & Reynard, N. S. (2009). Use of soil data in a grid-based hydrological model to estimate spatial variation in changing flood risk across the UK. *Journal of Hydrology*, *377*(3–4), 335–350. https://doi.org/10.1016/j.jhydrol.2009.08.031

Bierkens, M. F. P., Bell, V. A., Burek, P., Chaney, N., Condon, L. E., David, C. H., de Roo, Ad., Döll, P., Drost, N., Famiglietti, J. S., Flörke, M., Gochis, D. J., Houser, P., Hut, R., Keune, J., Kollet, S., Maxwell, R. M., Reager, J. T., Samaniego, L., … Wood, E. F. (2015). Hyper-resolution global hydrological modelling: What is next? "Everywhere and locally relevant". *Hydrological Processes*, *29*, 310–320.

Boughton, W. (2006). Calibrations of a daily rainfall-runoff model with poor quality data. *Environmental Modelling and Software*, *21*, 1114–1128.

Calder, I. R., Harding, R. J., & Rosier, P. T. W. (1983). An objective assessment of soil-moisture deficit models. *Journal of Hydrology*, *60*, 329–355.

Coppola, E., Sobolowski, S., Pichelli, E., Raffaele, F., Ahrens, B., Anders, I., Ban, N., Bastin, S., Belda, M., Belusic, D., Caldas-Alvarez, A., Cardoso, R. M., Davolio, S., Dobler, A., Fernandez, J., Fita, L., Fumiere, Q., Giorgi, F., Goergen, K., … Warrach-Sagi, K. (2020). A first-of-its-kind multi-model convection permitting ensemble for investigating convective phenomena over Europe and the Mediterranean. *Climate Dynamics*, *55*, 3–34.

Coxon, G., Freer, J., Lane, R., Dunne, T., Knoben, W. J., Howden, N. J., Quinn, N., Wagener, T., & Woods, R. (2019). DECIPHeR v1: Dynamic fluxEs and connectivity for predictions of HydRology. *Geoscientific Model Development*, *12*(6), 2285–2306.

Fiddes, J., & Gruber, S. (2014). TopoSCALE v.1.0: Downscaling gridded climate data in complex terrain. *Geoscientific Model Development*, *7*, 387–405.

Formetta, G., Prosdocimi, I., Stewart, E., & Bell, V. (2018). Estimating the index flood with continuous hydrological models: An application in Great Britain. *Hydrology Research*, *49*, 123–133.

Früh, B., Schipper, J. W., Pfeiffer, A., & Wirth, V. (2006). A pragmatic approach for downscaling precipitation in alpine-scale complex terrain. *Meteorologische Zeitschrift*, *15*(6), 631–646.

Gagnon, P., Rousseau, A. N., Mailhot, A., & Caya, D. (2012). Spatial disaggregation of mean areal rainfall using Gibbs sampling. *Journal of Hydrometeorology*, *13*(1), 324–337.

Hough, M. N., & Jones, R. J. A. (1997). The United Kingdom meteorological office rainfall and evaporation calculation system: MORECS version 2.0—An overview. *Hydrology and Earth System Sciences*, *1*, 227–239.

Kara, F., & Yucel, I. (2015). Climate change effects on extreme flows of water supply area in Istanbul: Utility of regional climate models and downscaling method. *Environmental Monitoring and Assessment*, *187*, 580.

Kay, A. L. (2021). Simulation of river flow in Britain under climate change: Baseline performance and future seasonal changes. *Hydrological Processes*, *35*(4), e14137. https://doi.org/10.1002/hyp.14137

Kay, A. L. (2022). Differences in hydrological impacts using regional climate model and nested convection-permitting model data. *Climatic Change*, *173*(1-2), 11. https://doi.org/10.1007/s10584-022-03405-z

Kay, A. L., Bell, V. A., Blyth, E. M., Crooks, S. M., Davies, H. N., & Reynard, N. S. (2013). A hydrological perspective on evaporation: Historical trends and future projections in Britain. *Journal of Water and Climate Change*, *4*(3), 193–208.

Kay, A. L., Booth, N., Lamb, R., Raven, E., Schaller, N., & Sparrow, S. (2018). Flood event attribution and damage estimation using national-scale grid-btased modelling: Winter 2013/14 in Great Britain. *International Journal of Climatology*, *38*(14), 5205–5219. https://doi.org/10.1002/joc5721

Kay, A. L., & Crooks, S. M. (2014). An investigation of the effect of transient climate change on snowmelt, flood frequency and timing in northern Britain. *International Journal of Climatology*, *34*(12), 3368–3381.

Kay, A. L., Davies, H. N., Lane, R. A., Rudd, A. C., & Bell, V. A. (2021). Grid-based simulation of river flows in Northern Ireland: Model performance and future flow changes. *Journal of Hydrology: Regional Studies*, *38*, 100967.

Kay, A. L., Reynard, N. S., & Jones, R. G. (2006). RCM rainfall for UK flood frequency estimation. I. Method and validation. *Journal of Hydrology*, *318*, 151–162.

Keller, V. D. J., Tanguy, M., Prosdocimi, I., Terry, J. A., Hitt, O., Cole, S. J., Fry, M., Morris, D. G., & Dixon, H. (2015). CEH-GEAR: 1 km resolution daily and monthly areal rainfall estimates for the UK for hydrological and other applications. *Earth System Science Data*, *7*, 143–155.

Kendon, E., Short, C., Pope, J., Chan, S., Wilkinson, J., Tucker, S., Bett, P., & Harris, G. (2021). *Update to UKCP local (2.2 km) projections*. Met Office Hadley Centre.

Kleinn, J., Frei, C., Gurtz, J., Luthi, D., Vidale, P. L., & Schar, C. (2005). Hydrological simulations in the Rhine Basin driven by regional climate models. *Journal of Geophysical Research*, *110*, D04102.

Lane, R. A., Coxon, G., Freer, J., Seibert, J., & Wagener, T. (2022). A large-sample investigation into uncertain climate change impacts on high flows across Great Britain. *Hydrology and Earth System Sciences*, *26*, 5535–5554.

Lane, R. A., & Kay, A. L. (2021). Climate change impact on the magnitude and timing of hydrological extremes across Great Britain. *Frontiers in Water*, *3*, 684982.

Maina, F. Z., Siirila-Woodburn, E. R., & Vahmani, P. (2020). Sensitivity of meteorological-forcing resolution on hydrologic variables. *Hydrology and Earth System Sciences*, *24*, 3451–3474.

Mamalakis, A., Langousis, A., Deidda, R., & Marrocu, M. (2017). A parametric approach for simultaneous bias correction and high-resolution downscaling of climate model rainfall. *Water Resources Research*, *53*(3), 2149–2170.

Manning, L. J., Hall, J. W., Fowler, H. J., Kilsby, C. G., & Tebaldi, C. (2009). Using probabilistic climate change information from a multimodel ensemble for water resources assessment. *Water Resources Research*, *45*, W11411.

Marke, T., Mauser, W., Pfeiffer, A., & Zängl, G. (2011). A pragmatic approach for the downscaling and bias correction of regional climate simulations: Evaluation in hydrological modelling. *Geoscientific Model Development*, *4*, 759–770.

Martinez-de la Torre, A., Blyth, E. M., & Robinson, E. L. (2018). Water, carbon and energy fluxes simulation for Great Britain using the JULES land surface model and the climate hydrology and ecology research support system meteorology dataset (1961-2015) [CHESS-land]. *NERC Environmental Information Data Centre*. https://doi.org/10.5285/c76096d6-45d4-4a69-a310-4c67f8dcf096

Marx, A., Pan, M., Rakovec, O., Samaniego, L., Sheffield, J., Wood, E. F., & Zink, M. (2018). Multi-model ensemble projections of European river floods and high flows at 1.5, 2, and 3 degrees global warming. *Environmental Research Letters*, *13*, 014003.

Met Office Hadley Centre. (2019). *UKCP local projections on a 5km grid over the UK for 1980-2080*. Centre for Environmental Data Analysis.

Met Office, Hollis, D., McCarthy, M., Kendon, M., Legg, T., & Simpson, I. (2019). *HadUK-grid gridded climate observations on a 1km grid over the UK, v1.0.0.0 (1862-2017)*. Centre for Environmental Data Analysis. https://doi.org/10.5285/2a62652a4fe6412693123dd6328f6dc8

Murphy, J. M., Harris, G. R., Sexton, D. M. H., Kendon, E. J., Bett, P. E., Clark, R. T., Eagle, K. E., Fosser, G., Fung, F., Lowe, J. A., McDonald, R. E., McInnes, R. N., McSweeney, C. F., Mitchell, J. F. B., Rostron, J. W., Thornton, H. E., Tucker, S., & Yamazaki, K. (2018). *UKCP18 land projections: Science report*. Met Office Hadley Centre.

Oudin, L., Michel, C., & Anctil, F. (2005). Which potential evapotranspiration input for a lumped rainfall-runoff model? Part 1 – Can rainfall-runoff models effectively handle detailed potential evapotranspiration inputs? *Journal of Hydrology*, *303*, 275–289.

Perra, E., Viola, F., Deidda, R., Caracciolo, D., Paniconi, C., & Langousis, A. (2020). Hydrologic impacts of surface elevation and spatial resolution in statistical correction approaches: Case study of Flumendosa Basin, Italy. *Journal of Hydrologic Engineering*, *25*(9), 05020032.

Pope, J. O., Brown, K., Fung, F., Hanlon, H. M., Neal, R., Palin, E. J., & Reid, A. (2022). Investigation of future climate change over the British Isles using weather patterns. *Climate Dynamics*, *58*, 2405–2419.

Prudhomme, C., Dadson, S., Morris, D., Williamson, J., Goodsell, G., Crooks, S., Boelee, L., Davies, H., Buys, G., Lafon, T., & Watts, G. (2012). Future flows climate: An ensemble of 1-km climate change projections for hydrological application in Great Britain. *Earth System Science Data*, *4*, 143–148.

Robinson, E. L., Blyth, E. M., Clark, D. B., Comyn-Platt, E., & Rudd, A. C. (2020a). *Climate hydrology and ecology research support system meteorology dataset for Great Britain (1961-2017) [CHESS-met]*. NERC EIDC. https://doi.org/10.5285/2ab15bf0-ad08-415c-ba64-831168be7293

Robinson, E. L., Blyth, E. M., Clark, D. B., Comyn-Platt, E., & Rudd, A. C. (2020b). *Climate hydrology and ecology research support system potential evapotranspiration dataset for Great Britain (1961-2017) [CHESS-PE]*. NERC EIDC. https://doi.org/10.5285/9116e565-2c0a-455b-9c68-558fdd9179ad

Robinson, E. L., Blyth, E. M., Clark, D. B., Finch, J., & Rudd, A. C. (2017). Trends in atmospheric evaporative demand in Great Britain using high-resolution meteorological data. *Hydrology and Earth System Sciences*, *21*, 1189–1224.

Robinson, E. L., Huntingford, C., Shamsudheen, V. S., & Bullock, J. M. (2022). *CHESS-SCAPE: Future projections of meteorological variables at 1 km resolution for the United Kingdom 1980-2080 derived from UK climate projections 2018*. NERC EDS CEDA. https://doi.org/10.5285/8194b416cbee482b89e0dfbe17c5786c

Rudd, A. C., Bell, V. A., & Kay, A. L. (2017). National-scale analysis of simulated hydrological droughts (1891-2015). *Journal of Hydrology*, *550*, 368–385.

Rudd, A. C., Kay, A. L., & Bell, V. A. (2019). National-scale analysis of future river flow and soil moisture droughts: Potential changes in drought characteristics. *Climatic Change*, *156*(3), 323–340.

Sampson, A. A., Wright, D. B., Stewart, R. D., & LoBue, A. C. (2020). The role of rainfall temporal and spatial averaging in seasonal simulations of the terrestrial water balance. *Hydrological Processes*, *34*(11), 2531–2542.

Schipper, J. W., Frueh, B., Pfeiffer, A., & Zaengl, G. (2011). Wind direction-dependent statistical downscaling of precipitation applied to the upper Danube catchment. *International Journal of Climatology*, *31*, 578–591.

Sharifi, E., Saghafian, B., & Steinacker, R. (2019). Downscaling satellite precipitation estimates with multiple linear regression, artificial neural networks, and spline interpolation techniques. *Journal of Geophysical Research: Atmospheres*, *124*, 789–805.

Sharma, D., Das Gupta, A., & Babel, M. S. (2007). Spatial disaggregation of bias-corrected GCM precipitation for improved hydrologic simulation: Ping River Basin, Thailand. *Hydrology and Earth System Sciences*, *11*, 1373–1390.

Skaugen, T. (2002). A spatial disaggregation procedure for precipitation. *Hydrological Sciences Journal*, *47*(6), 943–956.

Skoulikaris, C., Venetsanou, P., Lazoglou, G., Anagnostopoulou, C., & Voudouris, K. (2022). Spatio-temporal interpolation and bias correction ordering analysis for hydrological simulations: An assessment on a Mountainous River Basin. *Water*, *14*, 660.

Tanguy, M., Dixon, H., Prosdocimi, I., Morris, D. G., & Keller, V. D. J. (2016). *Gridded estimates of daily and monthly areal rainfall for the United Kingdom (1890–2015) [CEH-GEAR]*. NERC Environ. Inf. Data Centre. https://doi.org/10.5285/33604ea0-c238-4488-813d-0ad9ab7c51ca

Tian, J., Liu, J., Wang, Y., Wang, W., Li, C., & Hu, C. (2020). A coupled atmospheric–hydrologic modeling system with variable grid sizes for rainfall–runoff simulation in semi-humid and semi-arid watersheds: How does the coupling scale affects the results? *Hydrology and Earth System Sciences*, *24*, 3933–3949.

Yang, C., Chandler, R. E., Isham, V. S., Annoni, C., & Wheater, H. S. (2005). Simulation and downscaling models for potential evaporation. *Journal of Hydrology*, *302*, 239–254.

SUPPORTING INFORMATION

Additional supporting information can be found online in the Supporting Information section at the end of this article.

How to cite this article: Kay, A. L., Rudd, A. C., & Coulson, J. (2023). Spatial downscaling of precipitation for hydrological modelling: Assessing a simple method and its application under climate change in Britain. *Hydrological Processes*, *37*(2), e14823. https://doi.org/10.1002/hyp.14823